FP7 - 5:00

Identification for Robust Control of Flexible Structures

Gary J. Balas

Graduate Aeronautical Laboratories
California Institute of Technology
Pasadena, Ca. 91125

John C. Doyle

Dept. of Electrical Engineering
California Institute of Technology
Pasadena, Ca. 91125

Abstract

An accurate multivariable transfer function model of an experimental structure is required for research involving robust control of flexible structures. Initially, a multi-input/multi-output model of the structure is generated using the finite element method. This model was insufficient due to its variation from the experimental data. Therefore, Chebyshev polynomials are employed to fit the data with a single-input/multi-output transfer function models. Combining these lead to a multivariable model with more modes than the original finite element model. To find a physically motivated model, an ad hoc model reduction technique which uses a priori knowledge of the structure is developed. The ad hoc approach is compared with balanced realization model reduction to determine its benefits. Plots of select transfer function models and experimental data are included.

1 Introduction

This paper documents our experience with modeling and identification of a flexible structure for the purposes of control design. There are no new theoretical results in the paper, only application of curve fitting and model reduction techniques. These techniques provide an ad hoc approach to system identification, though a more systematic method is desired. We will try to motivate some important research directions in this area.

Initially, a theoretical model of the flexible structure is developed using the finite element method. The natural frequencies and modes shapes of the model vary considerably from the experimental data. These variations are attributed to inaccuracies in the modeling of interaction between the actuators and the structure, and to a lesser extent, the modeling of the joints in the structure.

Chebyshev polynomial curve fitting is used to formulate single-input/multi-output (SIMO) transfer function models from experimental data to provide more accurate models. A multi-input/multi-output (MIMO) transfer function model is constructed from the individual Chebyshev SIMO models, with the resulting MIMO model having the same number of states as the sum of the states of each SIMO model. In most cases, this leads to a number of excess states in the MIMO model which are not motivated from the physics of the problem. A direct MIMO curve fitting method has been developed [DailLuk], but its implementation presents some numerical problems and is not used.

Two methods are used to construct a reduced order MIMO model from the SIMO models: 1) using physically motivated arguments to combine states of the system, 2) balanced truncation. These methods provide varying degrees of accuracy in approximating the experimental data. For use in control design, the variation between the experimental data and the model needs to be taken into account. If one were to assume that the uncertainty in the model was zero, the control designs based on these models would be unstable on the real system. Similarly, if the difference between the model and the experimental data is accounted for by pure additive noise, an unstable control design would also be synthesized. Therefore, parametric and unstructured uncertainty models for the system are developed in an ad-hoc fashion.

It is apparent that there are a number of shortcomings associated with these methods for modeling and identification of flexible structures for control design. Some of the issues in need of attention are:

1. More straightforward and direct MIMO modeling.
2. Identification methods which produce nominal models with both perturbations and noise. For control design, there is an explicit need for uncertainty models.
3. Better finite element models. Of particular importance is the problem of producing nominal and uncertain models using the finite element method. These are bound to be conservative, but they will be better than the those used herein in the initial control design.
4. Better connection between the finite element model and the identified model. There should be a way of incorporating post-identification models of the system into updating the finite element model of the system.

Progress in these areas will lead to a more integrated framework with which structural and control design for flexible structures can be better performed.

2 Objective

The objective of the Caltech flexible structure experiment is to examine active control techniques for vibration suppression of flexible structures. The performance requirement is to provide a significant amount of vibration attenuation between the open-loop and the closed-loop system. There exists a tradeoff between the accuracy of the transfer function model and the achievable performance of the system. The high performance specifications on the structure require an accurate transfer function model of the structure together with a tight description of the associated uncertainties.

The control design methodology to be employed most naturally uses frequency domain descriptions of the plant model, uncertainties and performance specifications. Therefore, transfer function models are developed to accurately describe the experimentally derived bode plot data in the frequency domain of interest. Once models are defined, their variation from the experimental data can be quantified and used to develop ad hoc uncertainty models which bound these variations.

A model reduction technique based on a priori knowledge of the system and singular value decomposition is developed to complement the SIMO Chebyshev curve fitting method. This technique provides an ad hoc approach for generating sufficiently accurate multivariable transfer function models of flexible structures. For comparison purposes, model reduction based on balanced realizations is included [Moore,Enns,Glover].

3 Experimental Flexible Structure

An experimental flexible structure was designed to include a number of attributes associated with large flexible space structures [BalDoy]. These include closely spaced and lightly damped modes, noncollocated sensors and actuators, and numerous modes in the controller crossover region. In addition to these considerations, the ability to expand the structure was a desired feature. Expandability provides a means for increasing the modal density in a frequency range of interest. Another objective was to design the structure to have poor performance with the implementation of a collocated velocity feedback law at the actuators. This requires that a multivariable control design methodology be used to achieve the specified performance requirements.

The initial experimental structure consists of two stories, three longerons (columns) and three noncollocated sensors and actuators. The first story columns are .838 m (33 in.) long with the second story columns measuring .759 m (29.9 in.) Including the platforms, the structure has a height of 1.651 m (65 in.). The two platforms are triangular in shape with a .406 m (16 in.) base and a height of .353 m (13.9 in.). A longeron is connected to a platform by a triangular mating fixture and three bolts. This allows for the easy addition of stories to the structure. All the longerons are shrunk fit and welded to the mating brackets to reduce the affect of the joint nonlinearities. Issues associated with joint nonlinearities are an area of future research. Current plans include expanding the structure to 5 stories.

The first story platform is a 9.52 mm (3/8 in.) thick plate of aluminum, weighing 2.36 kg (5.2 lbs), with diagonal mounting brackets for attachment of the actuator diagonals. The second (lower) story platform is a 6.35 mm (1/4 in.) thick plate of aluminum with mounting holes for three accelerometers, it weighs 1.55 kg (3.4 lbs). A small offset mass is located on the second story platform to lower the torsional natural frequencies. The entire structure hangs from a mounting structure fixed to the ceiling. The three actuators are attached to the mounting structure and act along the diagonals of the first story. Hanging the structure from the ceiling alleviates the problem of buckling of the longerons.

The individual stories are designed to have the same first bending mode natural frequencies as one another. This requires the stiffness to mass ratio of each story be the same. With this in mind, the second story columns of the truss structure are designed to have one fourth the bending stiffness of the first story columns. This allows the interaction of the two stories to decrease the first natural frequency of the combined structure without significantly spreading out the remaining modes. The other reason for this is associated with the poor performance of a collocated velocity feedback design. Since the two stories have similar first bending mode frequencies, which are close to the first combined structural bending mode frequencies, requiring the first story to be rigid would provide little reduction in the second floor motion for similar second story excitation. This would be similar to implementation of a collocated velocity feedback law at the actuators.

3.1 Voice Coil Actuators

The actuators are a voice coil type design, built by Northern Magnetics Inc., which output a force proportional to an input voltage. The actuators are rated at ± 2.73 kg (6 lbs) of force at ± 10 volts and have a bandwidth of approximately 60 Hz. Currently, tests are being performed to more accurately characterise the input/output relationship of the actuators.

3.2 Accelerometers

The sensors are Sunstrand QA-1400 accelerometers. These are mounted on the second (lower) story platform, located along the x-axis, y-axis and at 45 degrees to both axes. The accelerometers are extremely sensitive and have a flat frequency response between 0 and 200 Hz. The noise associated with them is rated at 0.05 % of the output at 0-10 Hz and 2 % at 10-100 Hz. The sensors are scaled for accelerations of approximately 0.016 g per volt. This provides a maximum ± 5 volts output at peak accelerations of the input disturbance. The accelerometer output is conditioned by a 100 Hz, 4^{th} order Butterworth filter [OppSch,Stout] prior to input into the A/D; this provides attenuation of the high frequency response and noise.

3.3 Modeling

A model of the structure which relates signals input to the system to outputs is needed for control design purposes. The synthesis of control laws utilizes transfer function and/or state space descriptions of the control inputs to sensor outputs. Initially, a theoretical model is developed from a finite element model (FEM), from which an input/output model is derived. In addition to the theoretical model, a transfer function model between the actuators and sensors is determined via the ad hoc technique presented in this paper. A state space model is then constructed.

The FEM of the experiment structure provides a first approximation to the natural frequencies and mode shapes of the structure [DesAbel]. The beam elements are treated as space frame elements having three translational and three rotational degrees of freedom at each node and a torsional stiffness and bending stiffness in two directions. The longerons and diagonals are circular bars which have the same bending stiffnesses in both directions. The longerons are modeled as having fixed-fixed ends due to the welding of their end connections.

The accelerometers, mounting brackets, platforms and additional masses on the structure are modeled as lumped masses. The inertia properties of each is taken into account in the finite element description. When the control system is not activated, the diagonals in the first story ride on the bearings of the voice coil actuators. The diagonals are directly connected to the permanent magnetics inside the voice coil actuators via a threaded rod. No force is exerted along the diagonals in the open loop configuration. The actuators are modeled as having free motion parallel to the diagonals, and fixed in the plane perpendicular to the diagonals. In actuality, the diagonals ride on bearings which exhibit some stiction, friction and free play. These factors lead to errors between the theoretically determined transfer functions and the experimentally determined ones. The bearings also cause the damping levels to vary with the excitation amplitude.

The most flexible directions of the experimental truss structure are associated with the plane perpendicular to the longerons (the vertical hanging axis). The degrees of freedom associated with vertical motion, along the longerons, are neglected in the analysis. These neglected degrees of freedom lead to higher frequency modes between 35 and 200 Hz, which are outside the 6 Hz bandwidth of the current control design objectives.

A total of 15 degrees of freedom are included in the finite element model. The first six global modes are of interest for control purposes. The first group of local modes, which involve bending of the longerons, are located in the frequency range of 37 to 43 Hz. Vibration attenuation of these modes is not designed for, but these modes are consider in the control design to insure that they are not destabilized.

The following is a list of natural frequencies derived from the Nastran finite element model and natural frequencies and damping experimentally derived.

Damping Ratios and Natural Frequencies of the Caltech Experiment

Mode	NASTRAN Natural Frequency (Hz)	Experimental Natural Frequency (Hz)	Experimental Damping Ratio	Mode Type
1	.991	1.17	1.8 %	*1st* bending
2	.992	1.19	1.8 %	*1st* bending
3	2.004	2.26	1.0 %	*1st* torsional
4	2.069	2.66	1.6 %	*2nd* bending
5	2.100	2.75	1.8 %	*2nd* bending
6	3.832	4.43	0.9 %	*2nd* torsional

4 Experimental Transfer Functions

A more accurate input/output description of the structure can be derived experimentally. A white noise random process is used as an input signal to each voice coil actuator, with the accelerations due to this signal measured by the sensors. The accelerations are scaled to achieve a large signal to noise ratio for the disturbance excitation. With this in mind, the random noise signals are scaled accordingly. This leads to a maximum force output from the actuators of ±0.5 lbs for the noise input. The input signal, in the form of a voltage level, is output by the Masscomp computer D/A converters to each voice coil actuator. The corresponding signals from the sensors are filtered by a 100 Hz, 4^{th} order Butterworth filter [OppSch,Stout], and input to the Masscomp computer via the A/D converters. A sample rate of 200 Hz is used for the identification experiments, the same as in the closed-loop control experiments. Each single input to multi-output identification experiment is run for a total of 409.6 seconds (81,920 sample points).

A Fourier transform of the time history is performed on each input/output pair. For the Fourier transform, the data is chopped into windows of length 4096 data points. Each window overlaps the previous one by 2048 data points. A total of 39 windows of data is averaged for each transfer function. Hamming windowing is used on the time domain data to improve the smoothing properties of the frequency spectrum. A total of nine transfer functions are determined. The Bode plots of four experimentally derived transfer functions are shown in figures 1 and 2 together with the bode plots of the finite element transfer function models. In the plots of the FEM transfer functions, we have substituted the experimentally derived natural frequencies and damping ratios of the structure for the Nastran ones. The acronym in the title AiSj means from actuator i to sensor j.

One will notice that the agreement is poor between the theoretical finite element model and the experimental data in the frequency range of interest 0.5 to 5.5 Hz (3.14 to 34.5 rad/s). This discrepancy is likely due to inaccurate modeling of the interaction between the voice coil actuators and the diagonal elements of the structure and the longeron joints. This conjecture is based on the fact that all other component properties of the structure have been quantified and measured

The FEM had unacceptable variations from the experimental data. Therefore, new models are developed from the experimental data to more accurately represent the input/output behavior of the real system. The improved transfer functions model will be used to design active control systems for vibration suppression.

5 Chebyshev Polynomial Curve Fitting

Chebyshev polynomials have previously been used in FFT signal analyzers to curve fit measured transfer function data of single input/single output (SISO) systems [Adcock]. This technique was extended to single input/multiple output (SIMO) systems and has been applied successfully to experimental data [DailLuk]. The same technique is employed to develop SIMO transfer function models for the Caltech flexible structure experiment. A MIMO model is derived from the sum of the individual SIMO models. This model has twice the number of modes as the finite element model.

The transfer function equation,

$$g(s) = \frac{n(s)}{d(s)} = \frac{n_0 + n_1 s + n_2 s^2 + \cdots + n_N s^N}{d_0 + d_1 s + d_2 s^2 + \cdots + d_N s^N} \tag{1}$$

which is nonlinear in the coefficients, is transformed into a linear equation by multiplying through by the denominator, $g(s)d(s) - n(s) = 0$. The transfer function data is a set of complex numbers, $g(\jmath\omega)$, at various frequency points, ω. Separating this equation into real and imaginary parts, two real equations are produced for each value of ω. Written in matrix form, they form a linear least squares problem, $\inf_{\|x\|=1} \| \hat{A}x \|$. The real vector, x, contains the polynomial coefficients of $n(s)$ and $d(s)$.

A problem with this approach is that the matrix $\hat{A}$ is ill-conditioned. This is due to the ratio of $n(s)/d(s)$ being very sensitive to small changes in their coefficients. To alleviated this problem, the numerator and denominator are written as sums of Chebyshev polynomials and, therefore, indirectly as sums of powers of s, where s is define as $\jmath\omega$ [Adcock].

The numerator, $n(s)$, and denominator, $d(s)$, can be written as the sum of Chebyshev polynomials, and describing the transfer function data, $g(\jmath\omega)$, by its real and imaginary parts, $g(\jmath\omega) = g_r(\omega) + \jmath g_i(\omega)$, a matrix equation can be formed from the real and imaginary parts of the equation $g(\jmath\omega)d(\jmath\omega) - n(\jmath\omega) = 0$.

At each frequency point ω, the equation $g(\jmath\omega)d(\jmath\omega) - n(\jmath\omega)$ contributes two rows to the matrix $\hat{A}$. A weighting can be associated with each individual frequency point, allowing for accuracy of the fit to be traded off in different frequency ranges. Each row is normalized by $| g(\jmath\omega)d(\jmath\omega) |$, using an estimated $d(\jmath\omega)$ to achieve a constant relative accuracy (in log magnitude and phase) at each frequency.

The algorithm used to fit the data with Chebyshev polynomials is as follows [DailLuk]:

1. Read in data points, $g(\jmath\omega)$, and associated weights
2. Construct $A = \hat{A}^T\hat{A}$
3. Solve for x to minimize $x^T A x$
4. Use x to build $d(\jmath\omega)$, $n(\jmath\omega)$
5. Use $| g(\jmath\omega)d(\jmath\omega) |^{-1}$ as a weight, cycle back to Step 2
6. When the process converges, compute the state space realization of $n(s)/d(s)$

For the SIMO case, the denominator has the same dynamics as in the SISO case. Therefore, by extending the number of numerator coefficients, $n(s)$, one can address the SIMO case in a fashion similar to the SISO case. One problem with the Chebyshev curve fitting method is that it does not guarantee that a stable transfer function will be fit to the raw data. However, given that the frequency domain data reflects a stable system, and the polynomial approximation is a good fit to the data, the stability properties of the two are usually comparable. All of the structural transfer function are stable and the Chebyshev SIMO models have the same stability properties. Once the single input/multi-output transfer functions are fit with Chebyshev polynomials, the models are converted to a state space description.

6 MIMO Transfer Function Model

A multivariable transfer function model is constructed from the individual SIMO models. This model has the same number of states as the sum of each SIMO model, which leads to an excess number of states in the MIMO model which are not physically motivated. A SVD model reduction technique, based on an a priori model of the system, is developed to produce a MIMO transfer function model of the same order as the finite element model. The Chebyshev polynomial curve fitting and SVD based model reduction techniques are used in sequence to form a system identification method for flexible structures.

Based on the finite element model and physical data, the experimental structure has only six natural frequencies and mode shapes between 0.5 to 5.5 Hz. This is the frequency range in which an accurate multivariable model of the structure is required for control design. Therefore, the 3 input, 3 output multivariable transfer function model of the structure should have six modes associated with it. The SIMO Chebyshev curve fitting technique is used to develop transfer function models from each actuator to the three accelerometer sensors. These models contribute 4 modes to the total system model for each input. Although all six modes are excited by each actuator, only four modes appear distinctly in the experimental data. After fitting the individual SIMO transfer functions, 12 modes comprise the 3 input/3 output transfer function model. One would like to take advantage of the physical knowledge of the problem to reduce the 12 mode model to a 6 mode model.

6.1 Ad Hoc Model Reduction Technique

This model reduction technique requires an a priori knowledge of the flexible structure experiment. Modes in the SIMO models are grouped together based on their natural frequencies and the theoretical model. Four groups of modes are defined in the frequency range of interest. These groups include the first bending modes, first torsional mode, second bending modes and the second torsional mode. SVD is used to reduce the modes present in the Chebyshev MIMO model, to the number of physically motivated modes.

The experimental structure has two first bending and second bending modes present in the frequency range of interest. The two modes associated with the first bending mode have approximately the same natural frequency as do the second bending modes. The bending modes have similar natural frequencies, but their mode shape are perpendicular to one another. In the individual transfer functions it is hard to differentiate between the individual bending modes with similar natural frequencies. In fitting the Chebyshev polynomial models to the experimental data, the first and second bending modes are treated as having only one mode each. Each SIMO model consists of one first bending mode, a first torsional mode, a second bending mode and a second torsional mode.

The MIMO model constructed from the three SIMO models contains 12 modes. Combining the SIMO Chebyshev polynomial transfer function models for actuator 1 and 2, a 2 input, 3 output 8 mode model is formed. Since there are two first and second bending modes, the coefficients associated with both the first and second bending modes remain in the model. Therefore, it contains two modes which are not physically motivated. It was found that each torsional mode in the 8 mode model has two nearly identical natural frequencies associated with it, accounting for the two extra modes. This is due to the torsional response showing up predominantly in both sets of transfer function from actuator 1 and 2 to the three sensors. From the physics of the problem, there is only one mode associated with each torsional natural frequency. A common one mode model for each torsional mode needs to be unraveled from the two SIMO transfer function models. To see how this might be done, a modal description of the experimental structure is constructed.

The voice coil actuators input a force to the structure and accelerations are measured. Assuming modal damping, a SISO transfer function model relating force input to acceleration output can be developed for individual modes. For the i^{th} mode, it has the form:

$$\frac{b_i c_i s^2}{s^2 + 2\zeta_i \omega_i s + \omega_i^2} \tag{2}$$

rewriting the transfer function in strictly proper form yields

$$b_i c_i - \frac{2s\zeta_i\omega_i b_i c_i + \omega_i^2 b_i c_i}{s^2 + 2\zeta_i\omega_i s + \omega_i^2} \tag{3}$$

Since ζ_i and ω_i are known from the Chebyshev polynominal models, all the parameters of the problem have been determined. One will notice that only the combined scalar $b_i c_i$ can be determined uniquely. This approach does not allow for the identification of the individual modal coefficients b_i, c_i associated with each mode. However, the identified coefficients are within a scalar transformation of the modal coefficients. An extension of this methodology to determine the modal coefficients is of interest but is not currently being pursued.

In most instances, more than one mode is present in a transfer function. The SISO transfer function models developed for the experimental structure each consist of 4 individual modes. Each scalar D, in the state space formulation, is the sum of the 4 individual modes constant parts. There is no unique way of decomposing this into the individual $b_i c_i$ components from D. One way to determine each $b_i c_i$ component is to replace s by $j\omega$ and evaluate the strictly proper transfer function associated with each individual mode at $\omega = 0$.

The transfer functions, written in state space form, are described by

$$G(s) = \left[\begin{array}{c|c} A & B \\ \hline C & D \end{array}\right] \doteq D + C(sI - A)^{-1}B \tag{4}$$

evaluating this transfer function description as $s \to 0$, gives $D + C(-A)^{-1}B$, which should be zero.

For an individual mode in a SISO transfer function, the state space representation is of the form

$$\begin{aligned} G(s) &= \left[\begin{array}{cc|c} 0 & 1 & 0 \\ -\omega_i^2 & -2\zeta_i\omega_i & b_i c_i \\ \hline \omega_i^2 & 2\zeta_i\omega_i & d_i \end{array}\right] \\ &= d_i - \frac{2s\zeta_i\omega_i b_i c_i + \omega_i^2 b_i c_i}{s^2 + 2\zeta_i\omega_i s + \omega_i^2} \end{aligned} \tag{5}$$

evaluating this equation at $s = 0$, the d_i component is disregarded, and scaling $-A$ by -1 leads to

$$C(A)^{-1}B = \frac{b_i c_i \omega_i^2}{\omega_i^2} = b_i c_i \tag{6}$$

The same idea can be applied to multiple input and output pairs with a single mode. Instead of a scalar, a full matrix would be determined. A priori it is known that there is only one or two modes present in the data at each modal natural frequency. In the case of the experimental truss structure, it is known that there are two first bending modes whose natural frequencies are close, one first torsional, two second bending modes with close natural frequencies and one second torsional mode. Using this information, a SVD of the matrix is performed and the dominate mode is kept for the torsional case and two are kept for the bending cases. For one mode, the maximum singular value and its associated right and left eigenvectors determine the b_i and c_i coefficients.

The singular value decomposition for an $n \times m$ matrix A [MorZaf], is given by

$$A = U\Sigma V^* = \sum_{i=1}^{K} \sigma_i(A) u_i v_i^* \tag{7}$$

where U and V are unitary matrices with column vectors denoted by, $U = (u_1, u_2, \ldots, u_n)$ and $V = (v_1, v_2, \ldots, v_m)$, Σ contains a diagonal nonnegative definite matrix Σ_1 of singular values arranged in descending order. The C matrix corresponding to the output direction of the mode is constructed from the maximum singular value and the unitary U matrix. For a single mode, the C matrix is given by $C = \sigma_1 u_1$, where C is a vector of the length of the number of outputs. The B matrix, constructed from the V matrix, is given by $B^T = v_1$, which is the right singular vector associated with the maximum eigenvalue. The matrix $B^T C$ has the corresponding $b_i c_j$ matrix elements associated with input i and output j. For multiple modes, the B and C vectors would be matrices of size (number of modes × number of inputs) and (number of outputs × number of modes) respectfully. These matrices could be derived in a similar fashion.

This approach is used to transform the 3 input, 3 output, 12 mode model developed from Chebyshev polynomials into a 3 input, 3 output, six mode model which agrees with the physical properties of the structure in the frequency range of interest. The three SIMO transfer function models have 3 modes describing the first bending modes, 3 modes for the first torsional mode, 3 modes describing the second bending modes, and 3 modes for the second torsional mode. Applying the SVD based reduction method to these modal groups led to the development of a six mode MIMO transfer function model of the experimental flexible structure with 2 first bending modes, a first torsional mode, two second bending modes and second torsional mode.

Presented in figures 3 and 4 is a comparison between the Bode plots of the transfer functions from: (a) The experimental data, (b) the SIMO Chebyshev polynomial model method and (c) the six mode MIMO method derived using the techniques described above. The frequency range of interest for fitting of the Chebyshev polynomial model is between 0.5 and 5.5 Hz (3.14 and 35 rad/s).

6.2 Balanced Model Reduction

The method of model reduction based on balancing is also applied to the 12 mode MIMO model constructed from the three Chebyshev

SIMO models. The objective is the same as before, to obtain a 6 mode model from the Chebyshev MIMO 12 mode model. This method requires no physical knowledge of the system it is trying to approximate.

The balanced model reduction technique computes a m^{th} order reduced model

$$G_m = C_m(sI - A_m)^{-1}B_m + D_m \tag{8}$$

of a possibly non-minimal n^{th} order system

$$G = C(sI - A)^{-1}B + D \tag{9}$$

such that

$$\|G(\jmath\omega) - G_m(\jmath\omega)\|_\infty \leq 2 \sum_{i=m+1}^{n} \sigma(i) \tag{10}$$

where $\sigma(i)$ are the square-roots of the eigenvalues of the controllability and observability grammians. These are also the Hankel singular values of $G(s)$ [Moore,Enns,Glover].

A 6 mode MIMO model is developed using this technique. The reduced order transfer function model matches the original 12 mode MIMO quite well. The corresponding natural frequencies and damping values closely match those in the Chebyshev model also. The corresponding Bode plots functions are shown in figures 3 and 4 and are compared therein to those from the Chebyshev models and the experimental data.

7 Experimental Data and Models

Three different multivariable models are developed for the experimental data in the frequencies range of interest. The first model, **SIMO**, is the Chebyshev SIMO transfer function model for each actuator input. A 12 mode MIMO model is developed by combining the three Chebyshev SIMO models. The second model, **MIMO**, is the reduced, six mode MIMO transfer function model formed using the ad hoc model reduction technique. The third model, **Balanced**, is a six mode MIMO model formed by applying balanced model reduction to the Chebyshev SIMO transfer function models.

As one would expect, the Chebyshev SIMO models provide the best fit to the experimental data. This is due to the other two models approximating the Chebyshev model. The poorest fit occurs in the Bode plot representing the transfer function between actuator 1 and sensor 3. Since actuator 1 excites the direction perpendicular to sensor 3, the magnitude of the transfer function is an order of magnitude below that of the other actuator 1 transfer functions. The curve fitting technique applies a maximum magnitude error criteria to fit the data which accounts for this discrepancy.

The ad hoc technique achieves a very good fit to all the experimental Bode plot data except from actuator 1 to sensor 3. The magnitude and phase characteristics of all the other Bode plots are well matched. Though, the Bode plots of this model do not fit the experimental data as well as the SIMO models. The balanced model reduction also fit the data well, with the notable exception of the Bode plots associated with the transfer functions of A2S2 and A1S3. The balanced model transfer function from actuator 2 to sensor 2 has problems with the interlacing of the poles and zeros associated with the second bending modes. Overall, the balanced model reduction method performed quite well considering it had no knowledge of the dynamic characteristics of the system. The ad hoc technique produced the best six mode model corresponding to the experimental data.

8 Conclusions

The finite element model of the structure provided a physical understanding of the dynamic characteristics of the first six modes. Unfortunately, this model had considerable error in the determination of the natural frequencies and mode shapes of the structure. To obtain a more accurate model of the experimental data, we employed Chebyshev polynomials to curve fit the data. This approach proved successful in deriving SIMO transfer function models for each actuator input which accurately fit the data in the frequency range of 0.5 to 5.5 Hz. To form a MIMO model, the three SIMO models were combined. A shortcoming of this was that additional modes were present in the model that were not physically motivated from the finite element analysis. The resulting Chebyshev MIMO model contained 12 modes whereas the finite element model had only six.

The ad hoc model reduction technique provided the best fit to the experimental data for a six mode model consistent with the finite element analysis. The balanced model reduction also provided a consistent model which fit the data. An a priori knowledge of the physical system aids in providing an accurate transfer function model corresponding to the physical data.

The problem with all three approaches is that they don't provide models which are readily useful for control design. A series of ad hoc assumptions and fixes are required to fit them into the robust control framework. The uncertainty models were determined from engineering judgement, not a systematic approach. It is therefore hard to verify their accuracy. As discussed in the introduction, there are a number of issues that need to be resolved in the area of identification for control design. Although the developed models proved very useful for our research, we have a great interest in approaching system identification in a manner more consistent with the robust control framework.

9 Acknowledgements

The authors would like to thank Dr. Harold Stalford for his input and Dr. R. Lane Dailey for the Chebyshev polynomial curve fitting software. The authors acknowledge financial support from the NASA Graduate Student Fellowship, and Caltech President's Fund.

10 References

Adcock J.L. Adcock, "Curve fitter for pole-zero analysis," Hewlett-Packard Journal, January, 1987.

BalDoy G.J. Balas and J.C. Doyle, "On the Caltech experimental large space structure," ACC, Atlanta, GA, June, 1988.

DailLuk R.L. Dailey and M.S. Lukich, "MIMO transfer function curve fitting using Chebyshev polynomials," SIAM 35*th* Anniv. Meeting, Denver, CO, 1987.

DesAbel Desai, C.S. and Abel, J.F., *Introduction to the Finite Element Method: A Numerical Method for Engineering Analysis*, Van Norstrand Reinhold Company, 1972.

Enns D. Enns, "Model reduction for control system design," Ph.D. dissertation, Stanford University, 1984.

Glover K. Glover, "All optimal Hankel norm approximations of linear multivariable systems and their L_∞ error bounds," Int. Journal of Control, 39, No. 6, 1984, pp 1115-1193.

Moore B.C. Moore, "Principal components analysis in linear systems: controllability, observability and model reduction," IEEE Proceedings on Automatic Control, Vol. AC-26, pp 17-31, Feb 1981.

MorZaf M. Morari and E. Zafiriou, *Robust Process Control*, Prentice-Hall, N.J., 1989.

OppSch A. Oppenheim and R.W. Schafer, *Digital Signal Processing*, Prentice-Hall, N.J., 1975.

Stout D.F. Stout, *Handbook of Operational Amplifiers Circuit Design*, McGraw-Hill, N.Y., 1976.

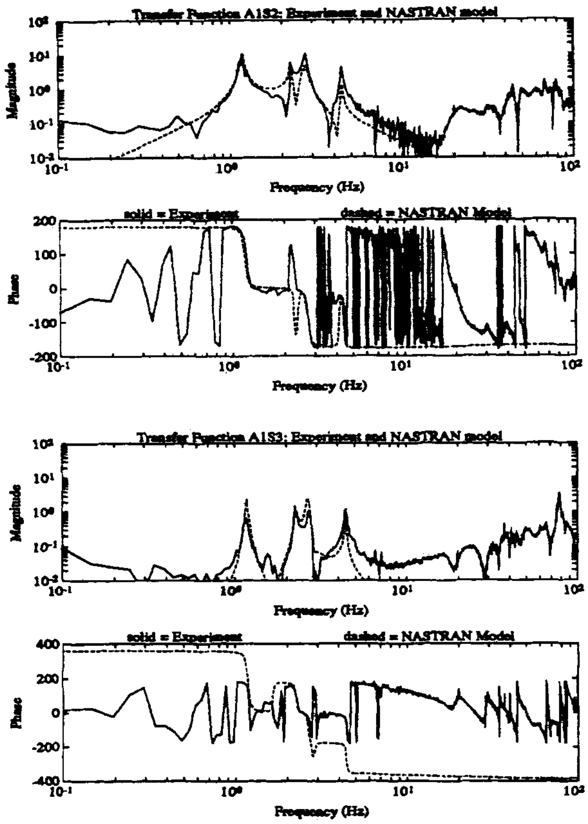

Figure 1: Transfer Functions A1S2 and A1S3

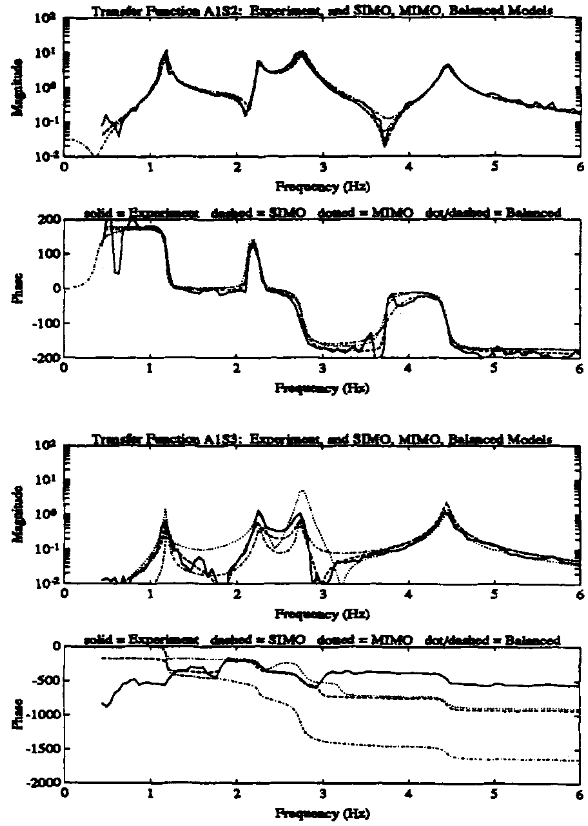

Figure 3: Transfer Functions A1S2 and A1S3

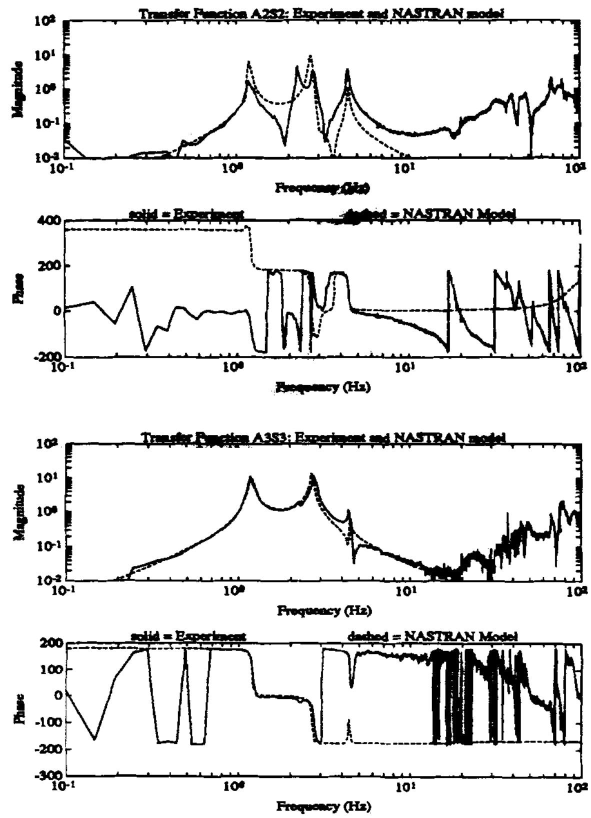

Figure 2: Transfer Functions A2S2 and A3S3

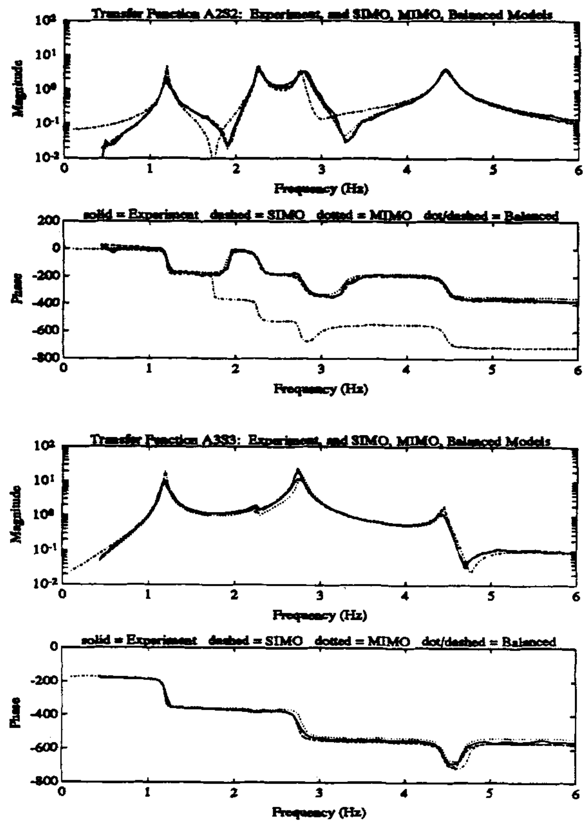

Figure 4: Transfer Functions A2S2 and A3S3